sciendo

Bulletin of Geography. Physical Geography Series, No. 18 (2020): 41–60
http://dx.doi.org/10.2478/bgeo-2020-0004

Variations in the bathymetry and bottom morphology of the Izu-Bonin Trench modelled by GMT

ISSN 2080-7686

OPEN ACCESS

Polina Lemenkova

Ocean University of China, College of Marine Geo-sciences, Qingdao, China

Correspondence: Ocean University of China, Qingdao, China. E-mail: pauline.lemenkova@gmail.com

https://orcid.org/0000-0002-5759-1089

Abstract. Cartographic visualisation is a central concept in geoinformatics, and Generic Mapping Tools (GMT) functionality provides a variety of modules for effective mapping. However, due to its specific scripting approach, there is not enough reported experience of GMT mapping, comparing to traditional GIS. This contribution introduces steps that can be taken to perform cartographic mapping and modelling using GMT. Geographically, this paper investigates the Izu-Bonin Trench in the Pacific Ocean. The aim was to compare its geomorphology in two segments, and each was modelled by a series of profiles. The comparative analysis shows that the southern segment is deeper and is a more precisely V-shaped form with a steeper gradient slope. The northern part has an asymmetric slope with submarine terraces to the west and a straight shape to the east. The northern profile is based on 407 samples (13.5%) at depths of -5,600 to -5,800 m, followed by 304 samples at -5,800 to -6,000 m (10%). The southern histogram has a bimodal distribution with two peaks: 523 samples (20%) with depths of -5,800 to -6,000 m. The second peak (10%) is on the Bonin Ridge. The GMT proved to be an effective instrument for marine geological mapping, 3D and 2D modelling, statistical analysis and graphical plotting.

Key words:
Izu-Bonin Trench,
GEBCO,
GMT,
Cartography,
Mapping,
Modelling,
Submarine Geomorphology,
Pacific Ocean

Introduction

The Izu-Bonin Trench, also known as the Izu-Ogasawara Trench, is a hadal trench in the west Pacific Ocean to the south of Japan (Fig. 1). Longitudinally, it extends from near Tokyo in Japan to Guam (Barnes and Straub 2010). In its structure, the trench continues the Japan Trench. Geographically, the Izu-Bonin Trench is bordered to the east by the Ogasawara Plateau (Nishizawa et al. 2006) stretching in the northern part of the Philippine Sea, which is bounded to the east by island arcs (Nanpō Islands, Mariana, Yap, Palau) and deep-sea trenches. The seafloor of the Philippine Sea is classified as "oceanic" type (Leont'ev 1968; Peyve 1980). It is divided by the submarine ridges into major basins: Philippine (dominating depths 5,500–5,800 m), Nampō and Western Mariana (4,800–5,200 m). The Kyushu-Palau chain of pointy steep-sided mountains (2,000–5,000 m) separates the Nampō and Western Mariana basins of the Philippine Sea (Litvin 1987). The seafloor relief in the Philippine Sea is strongly dissected and hilly, with depth amplitudes from 100 to 500–700 m. The orientation of the ridges is mainly sub-meridional and north-western, corresponding to its geomorphic structures. In the northern and western parts of the Philippine Basin, block elevations with large block dissections reach up to 4,000 m. In the east, it is limited to a sub-meridional, arched to the east ridge.

The Bonin Islands are located on the outer ridge, and the Volcano Islands on the inner ridge of the Nampō island arc. This system continues to the south as a double arc curved to the east with the Mariana Islands formed on its outer ridge. This entire system of ridges has a structure typical of island arcs (Rodnikov 1979). It has convex, stepped slopes with the lower parts steeper than the upper ones. The Izu-Bonin Trench stretches along the lower basement of these outer slopes. It continues to the Mariana Trench, which is separated from it by low threshold. The bottom of the trench's seafloor is flat and narrow, with a maximum depth of 9,780 m (Udintsev 1972).

The Izu-Bonin Trench is formed in the area of active tectonic subduction of the Cretaceous (135 Ma) Pacific Plate beneath the Philippine Sea Plate (Sano et al. 2016). As a consequence of this subduction the following structures are formed: the volcanic arc of the Izu and Bonin Islands on the Izu-Bonin-Mariana Arc system and the Shikoku Basin as a backarc basin (Fig. 2). In its development, the Izu-Bonin arc has two major periods of arc formation that differ in duration, composition, and volcanology. The first lasted ~5 to 6 million years and produced voluminous boninitic–tholeiitic magmas (Nakajima and Arima 1998). The second post-42 Ma period of the Izu-Bonin arc's formation produced a classical volcanic arc with stratocones (Barnes and Straub 2010).

Further geologic development of the Izu-Bonin arc and formation of the Shikoku backarc basin took place in the early Miocene, ~30–15 Ma (Cox 1973; Taylor 1992). It then continued during the Middle Miocene when the Philippine Sea Plate migrated north-westward (Whitman et al. 1983). As a consequence, the Izu-Bonin arc collided with the Honshu arc (Niitsuma 1989; Soh et al. 1991; Takahashi and Saito 1997). At the same time, the south-west Honshu arc rotated clockwise, which strengthened the collision of the arcs (Otofuji et al. 1994). As a result, the Izu-Bonin arc collided with the Honshu arc, together forming a globally unique active Izu arc–arc Collision Zone (ICZ) in central Japan (Arai and Iwasaki 2014). The collision resulted in Izu-Bonin arc crust accreting onto the Honshu arc, associated with movements of the tectonic plate and Izu-Bonin trench formation (Soh et al. 1998). A new period of along-strike arc rifting began about 2.5 Ma ago (Ishizuka et al. 2003). The development of the oceanic trench is mirrored in its seabed structure, which is well structured: a sedimentary cover, a basalt of tholeiitic composition (Reagan et al. 2010), a complex of parallel diabase dykes, gabbro and gabbro-ultrabasic complex lying on mantle ultrabasites (Lemenkova 2019b).

The trench extends to nearly 10 km depth. The 200-km wide forearc region includes an inner trench slope with a basal terrace and seamounts, an outer arc connected to the Bonin Islands and a thick forearc sedimentary basin east of the active arc volcanoes. The backarc region encompasses active rift basins and cross-chains of submarine arc volcanoes extending into the Shikoku Basin (DeBari et al. 1999). The northern end of the Izu-Bonin arc is a juvenile oceanic arc colliding with the Honshu arc, a mature island arc since the Middle Miocene (Stern et al. 2003). A chain of serpentine seamounts is exposed at the forearc slope 40–50 km west of the Izu-Bonin Trench axis. Seismically, few large earthquakes (>M7.0) (Kamimura et al. 2002) are detected at depths <100 km (red circles on Fig. 2) and many large earthquakes at depths 100–300 km (Fig. 2). The Boso triple junction located on the north of the Izu-Bonin Collision Zone (Fig. 2) is the northern end of the arc colliding with the Honshu Island arc as a consequence of the NW migration of the Philippine Sea Plate (Ogawa et al. 1989).

Many factors affect the structure of a hadal trench, its dynamics and present geomorphology (Lemenkova 2018a). The complexity of the processes taking place along subduction zones is illustrated by Woelki et al. (2018): where oceanic crust and sediment are recycled into the mantle, causing mantle melting and heterogeneity, arc magmatism, degassing and the creation of new continental crust. The trench is then formed where the tectonic plates are being subducted. The Izu-Bonin Trench is bordered by the Philippine Sea plate in the west. The Philippine Sea is a geologically complex region notable for its varied bathymetry and plate shape (Yamazaki et al. 2010) as well as its complex patchwork of seafloor ages. The bounding subduction zones of the Philippine Sea Plate exhibit significant N–S variation in slab morphology (Čížková and Bina 2015).

As a result of the interplay of these factors, the trench consists of the Izu (north) and the Bonin

 Citation: Bulletin of Geography. Physical Geography Series 2020, 18, http://dx.doi.org/10.2478/bgeo-2020-0004

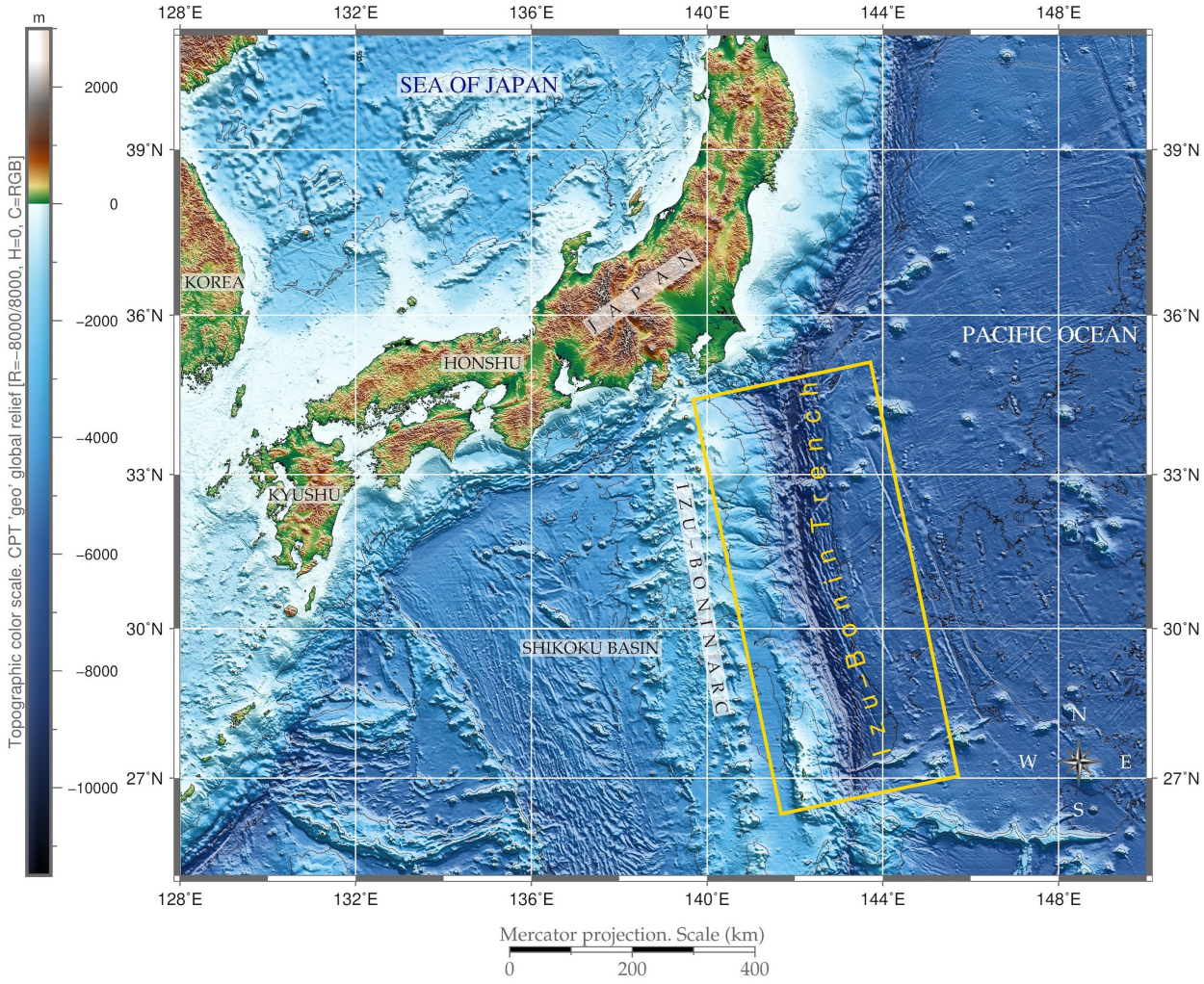

Fig. 1. Topographic map of the study area: Izu-Bonin Trench

(south) separated roughly by the Ogasawara Plateau. Thus, seafloor ageing affects the advancing trench through the subduction of progressively older and stiffer lithospheric material (Faccenna et al. 2009). Furthermore, Ishizuka et al. (2018) noted that the asymmetric spreading was caused by ridge migration in the Izu-Bonin region in view of the age difference between the oldest forearc basalt and the crust of the Amami Sankaku Basin. Other factors besides tectonic development, including, for instance, deep ocean currents that bring sediments to the trench bottom thus contributing towards the accumulation of the sediment thickness (Lemenkova 2019a), impact on the development of the lithosphere via a constant exchange of matter and energy between the submarine volcanoes.

More detailed descriptions of the geophysical, petrological and geochemical settings, volcanism and seismic characteristics, analysis and interpretation of geomorphological, geological, and thermochronological data of the Izu-Bonin tectonics are reported in relevant publications (Tuezov 1978; Kawate and Arima 1998; Dobson et al. 2006; Tamura et al. 2010; Tollstrup et al. 2010; Oshika et al. 2014; Arculus et al. 2015; Arisa and Heki 2016; Senda et al. 2016; Hashima et al. 2016; Ichiyama et al. 2017; Gong et al. 2018; Zhang et al. 2019). Hence, the region of the Izu-Bonin Arc is now one of the best and most intensively studied oceanic arcs. However, less attention has been given to the submarine geomorphology of the Izu-Bonin Trench as a deep-sea geomorphic structure. With regard to the lack of such research, the current study aims to further the understanding of the trench system by mapping and modelling its geomorphic form using the car-

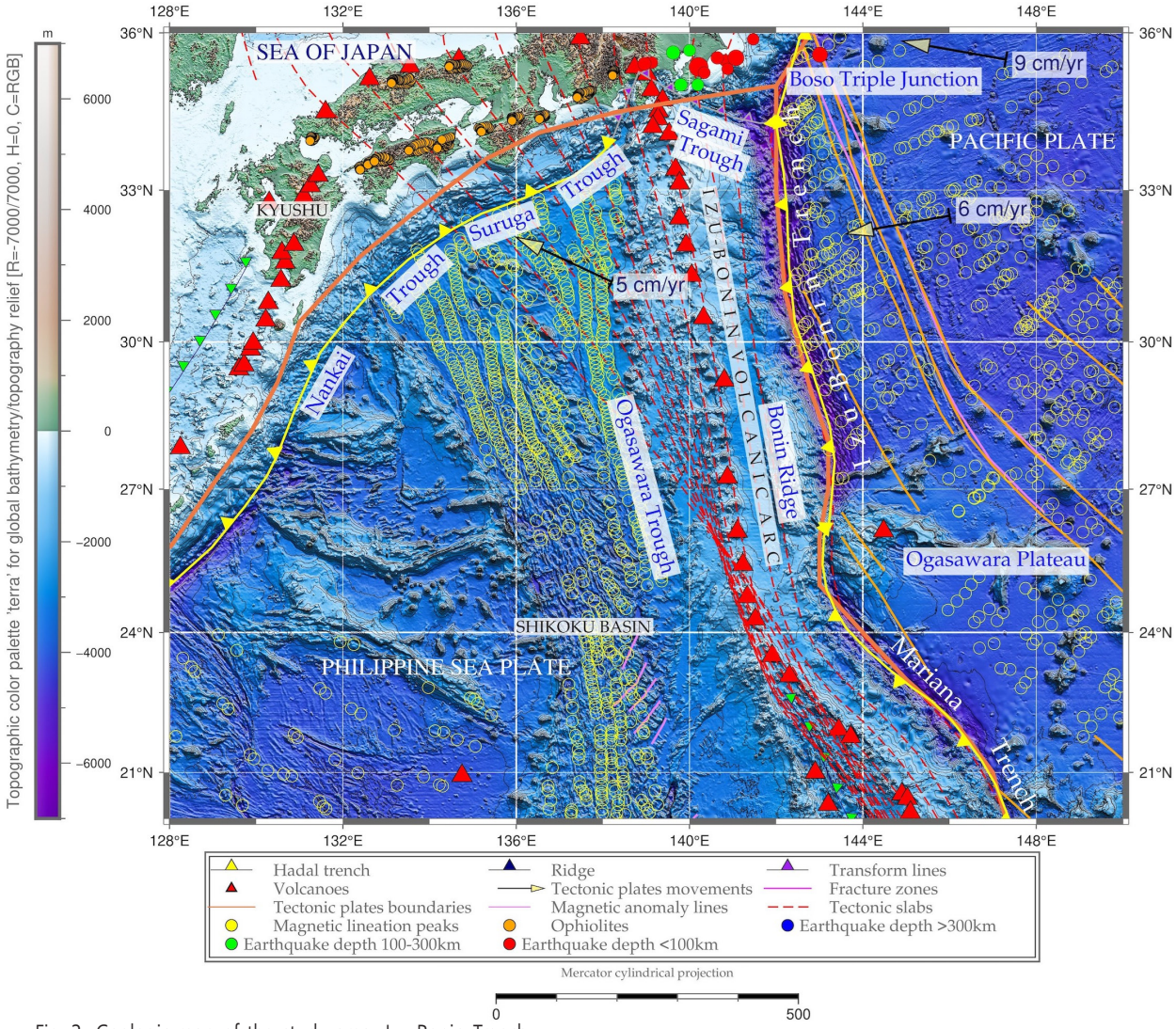

Fig. 2. Geologic map of the study area: Izu-Bonin Trench

tographic approach of the Generic Mapping Toolset (GMT).

Materials and methods

The primary goal of this research was to compare the geomorphology and slope steepness of two segments from the Izu-Bonin trench. Bathymetric cross-sectioned profiles (Fig. 7) show that the southern segment of the Izu-Bonin trench (Fig. 7B) has a steep outer slope and more precisely V-shaped cross-profile. The northern part of the trench (Fig. 7A) has seamounts on the eastern side (which can also be seen in Fig. 6) and submarine terraces.

Since bathymetric data accuracy is of highest importance (Smith 1993), the data for this study is based on the high-resolution bathymetric/topographic global data model for ocean and land, GEBCO (The General Bathymetric Chart of the Oceans): https://www.gebco.net/. The major advantage of GEBCO for bathymetric mapping lies in its accuracy. In general, the accuracy of the geospatial datasets appears to be higher on various data sets of increased resolution. Therefore, a GEBCO global terrain model at 15 arc-second intervals was selected as a major data source for plotting the maps in Figure 1, Figure 2 and Figure 6.

Citation: Bulletin of Geography. Physical Geography Series 2020, 18, http://dx.doi.org/10.2478/bgeo-2020-0004

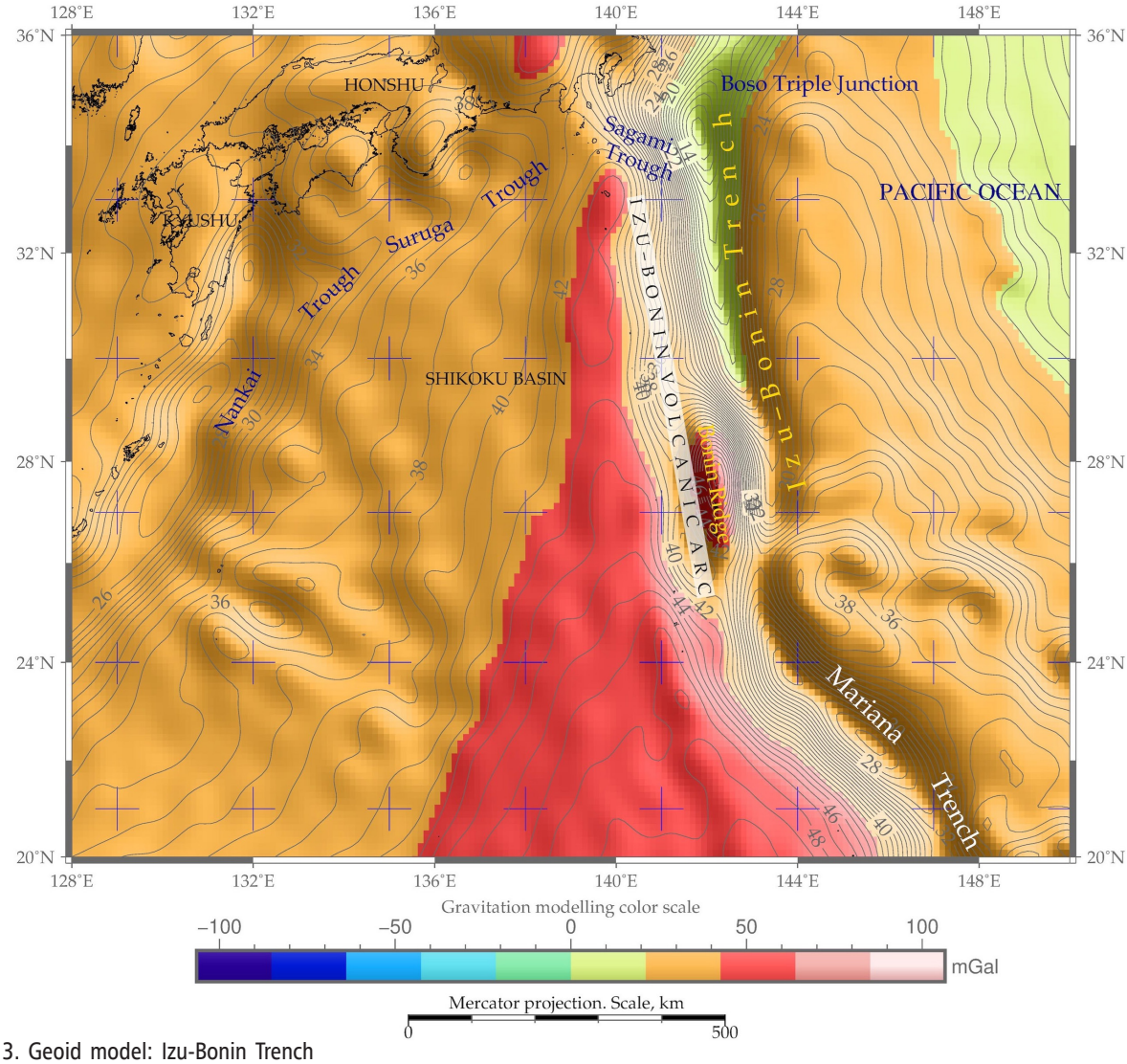

Fig. 3. Geoid model: Izu-Bonin Trench

The description of the GEBCO goals, ideas and general objectives of mapping can be found in the relevant publications of the GEBCO Committee (2016) and Weatherall et al. (2016). The GEBCO dataset grid is supported by ship-based cruises, which allows the high of accuracy in GEBCO grids to be maintained, resulting in its 15-arc-second resolution (Weatherall and Cramer 2004). The GEBCO project is focused on high-precision bathymetric mapping of the seafloor (Wyatt 2019). It originated in the early 20th century and is currently being developed by multiple oceanographic institutions. The use of the GEBCO grid here was facilitated through the GMT and the application of methodologies available for issues of bathymetric mapping (Hell and Jakobsson 2011) and documentation of GMT (Wessel and Smith 1998).

In response to the increasing requirements for cartographic quality and big data processing, various GIS have been developed during the last decades to meet needs in thematic and bathymetric mapping, e.g. ArcGIS, GRASS GIS, QGIS, MapInfo, Erdas Imagine, ENVI GIS, to mention a few. As one of the most popular GIS softwares, ArcGIS has been used and tested extensively in geospatial research (Suetova et al. 2005a; Kuhn et al. 2006; Lemenkova 2011; Lemenkova et al. 2012; Klaučo et al. 2017). GRASS GIS (Geographic Resources Analysis Support System) has most recently launched its version 7.8 (information on 25.04.2020) and is becoming increasingly popular as a free open source

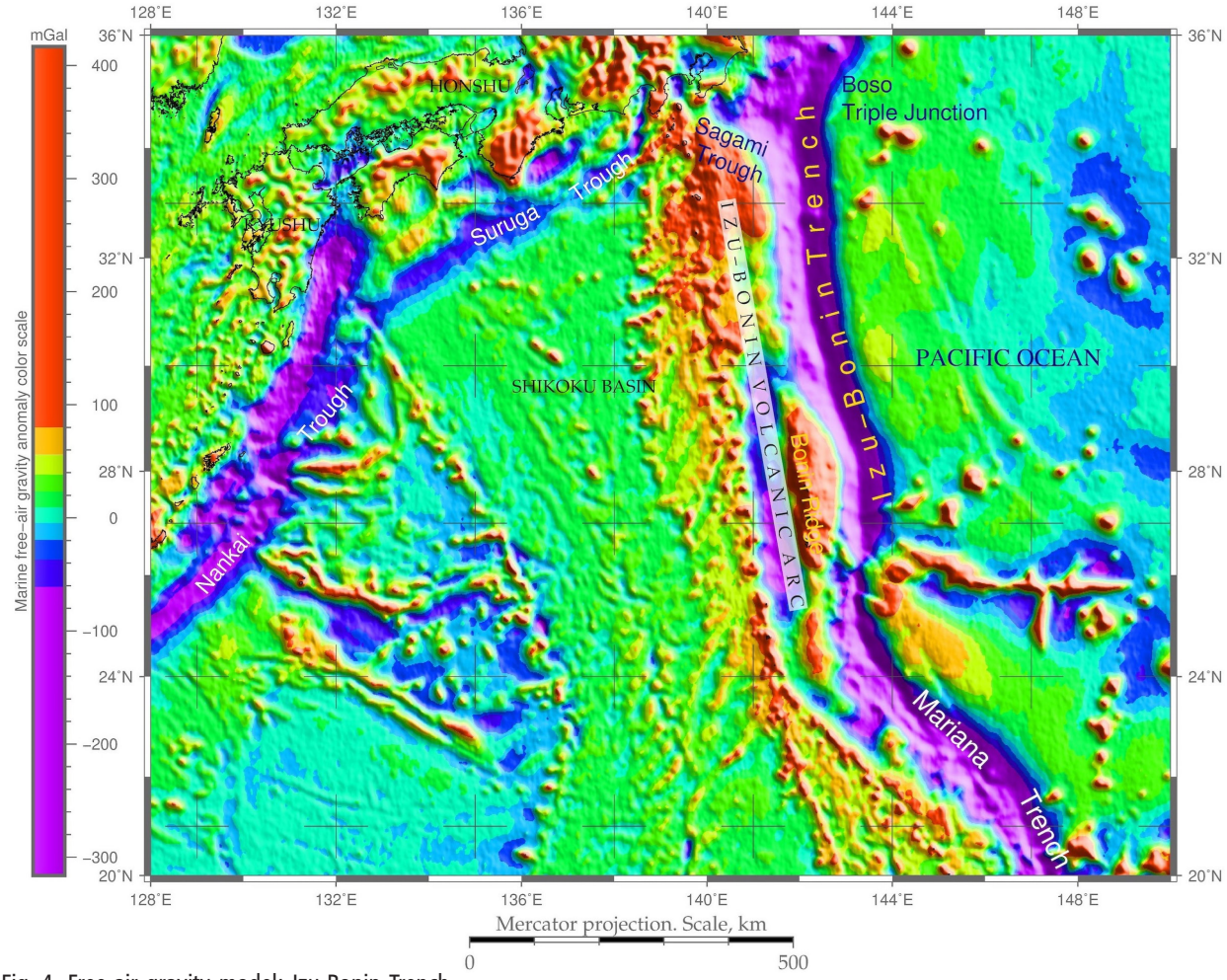

Fig. 4. Free-air gravity model: Izu-Bonin Trench

GIS with a GUI (Graphical User Interface) and a console. In Canada, the Teledyne CARIS developed CARIS (Computer Aided Resource Information System) software for marine mapping and raw bathymetric surveys. An example of a combination of ArcGIS and CARIS HIPS for swath bathymetric mapping followed by GMT data processing is given by Gauger et al. (2007).

The GMT nonetheless has certain advantages over the mentioned above GIS, in particular the scripting approach, automation of cross-section profiles, visualisation of high-quality raster grids, and full support of cartographic works (projection, design, geospatial analysis and queries, modelling, statistical analysis, layouts, printing). The main difference distinguishing GMT from other GIS is its performance of cartographic mapping through a console-based scripting approach in which each command of the scripting code roughly corresponds to an element or layer of the plotted map. Thereby, the resulting map in postscript format (.ps) is designed stepwise based on a set of the command lines. Cartographic elements are added to the final layout using GMT modules and their flags are important for code evaluation (attributes of fonts, colours, selection of algorithms of rad data processing, size and types of plotted symbols). For example, using GMT, selected pieces of raster grids can easily be subset from the initial raster grid, converted in terms of formats (GeoTIFF, NetCDF), and reprojected to a vast variety of cartographic projections specific to the selected map, without initialising a new GIS project (which ArcGIS requires).

The principle of thematic mapping by means of GMT consists in the following. The mapping "as is" is performed through the command line via running shell script. Each script contains a sequence of lines of codes. Similar in principle to program-

Citation: Bulletin of Geography. Physical Geography Series 2020, 18, http://dx.doi.org/10.2478/bgeo-2020-0004

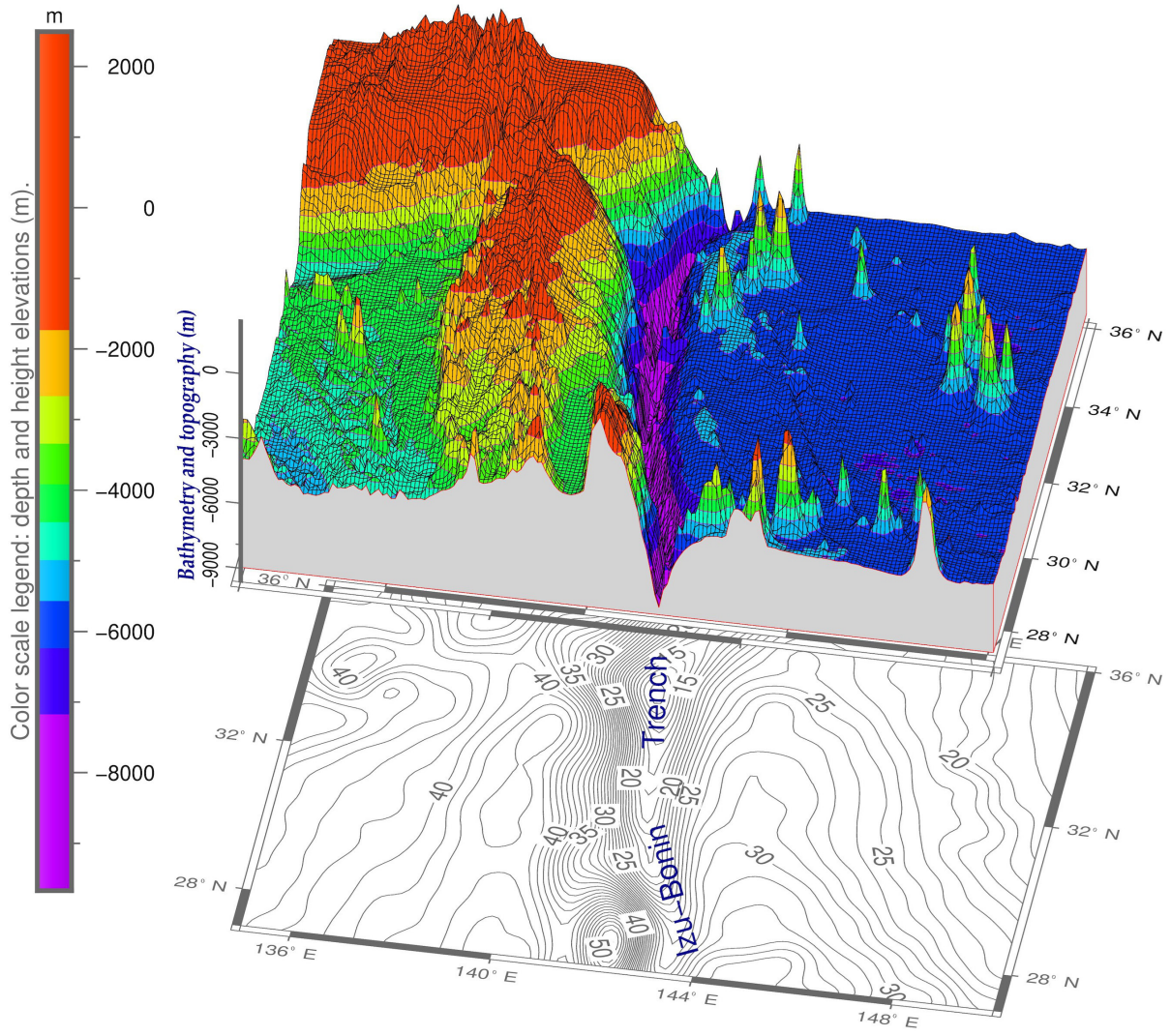

Fig. 5. 3D model of the study area: Izu-Bonin Trench

ming languages, the lines of the GMT codes are used to plot every cartographic element on the map including coast lines, grids, projection, embellishments, titles and subtitles, and texts. In this sense, the architecture of the GMT has a straightforward approach of "map-oriented" (not "project-oriented") mapping, in contrast to other GIS. Hence, through such advanced functionality, GMT responds to the need for quick and precise mapping based on large amounts of data. GMT enables effective and rapid data processing and manipulation with big datasets on geology and seabed topography (e.g. GEBCO), which results in high-quality bathymetric mapping and assists in spatial analysis of bottom morphology.

Geologic and geophysical mapping

There are multiple GMT modules that were used in the thematic mapping (Wessel et al. 2013). For example, the bathymetric/topographic map (Fig. 1) was plotted using a combination of the following modules: gmtset, gmtdefaults, grdcut, makecpt, grdimage, psscale, grdcontour, psbasemap, gmtlogo, psconvert. The geoid map (Fig. 3) was mapped using the following GMT modules: gmtset, grd2cpt, grdimage, pscoast, grdcontour, psbasemap, psscale, psimage, logo, pstext, psconvert. To be more specific, the example of the GMT code used for mapping free-air gravity map (Fig. 4) is provided below. The data for the marine free-air gravity and geoid models (Earth Gravitational Models, EGM96) were

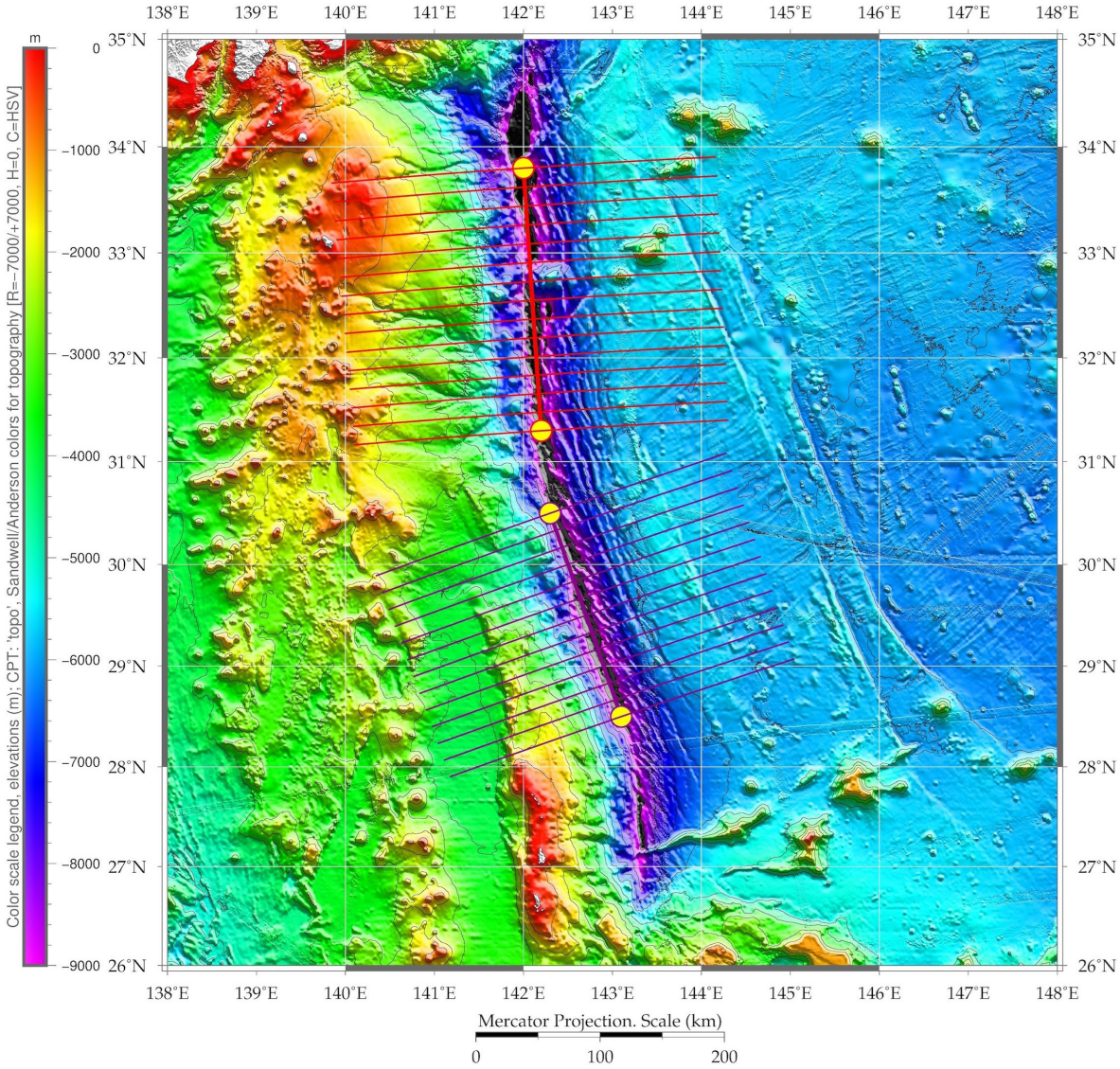

Fig. 6. Enlarged map of the selected fragment of digitised profiles: Izu-Bonin Trench

taken from the available grids (Smith and Sandwell 1995; Sandwell et al. 2014) of Scripps Institution of Oceanology. The resulting thematic maps are presented as Figures 2-4.

Cross-sectioning profiles for topographic modelling

Machine learning techniques have become important in GIS and geospatial analysis, as they are particularly suited to facilitating monotonous routine cartographic work, such as digitising (Schenke and Lemenkova 2008). Besides speed, modelling complex objects such as hadal trenches requires an algorithm of precise cross-section profiling that can produce reliable and accurate results.

The aim of the cross-sectioning in this study was to make two sets of bathymetric profiles in the northern and southern segments of the trench, and to sample the deepest values of both using GMT (Fig. 6). Because in its structure the northern part of the Izu-Bonin trench (the Izu Trench segment) bends gently by the Bonin Ridge extension (Fig. 6), the study suggested the comparison of the two segments on its northern and southern parts. Two transects of 400 km long, spaced 20 km apart and sampled by observations of depth every 2 km, were made on the northern part of the trench slope of the Izu-Bonin arc (Fig. 1) using "grdtrack", "con-

Citation: Bulletin of Geography. Physical Geography Series 2020, 18, http://dx.doi.org/10.2478/bgeo-2020-0004

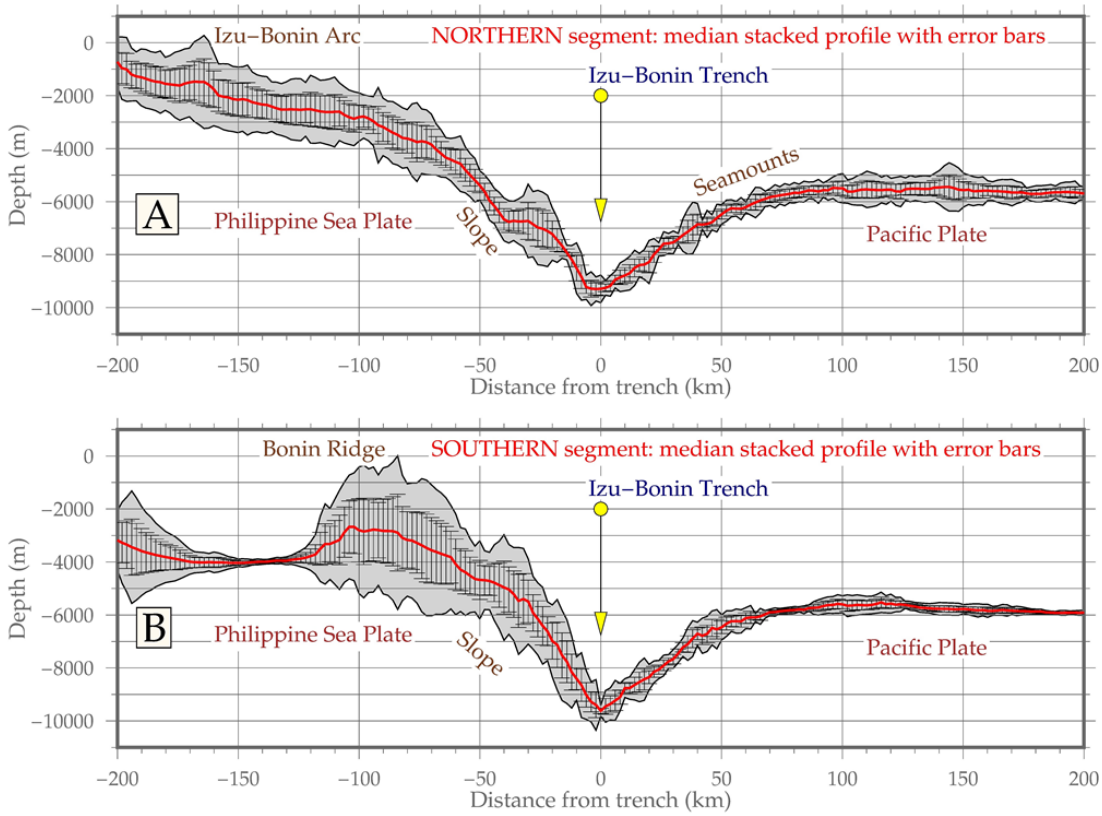

Fig. 7. Modelled graphs of the relief cross-section profiles of the Izu-Bonin Trench

vert" and "psxy" as the main GMT modules. The first segment stretches in an almost longitudinal direction with coordinates 142.2°E 31.3°N to 142.0°E 33.8°N. The second segment has a notable SE bending and the following coordinates: 143.1°E 28.5°N to 142.3°E 30.5°N. The profile used for cross-sectioning the trench was digitised in these two segments, respectively (Fig. 6). Technically, digitising of the transects and modelling of the geomorphic profiles were based on the methodology explained in GMT references (Wessel and Smith 2018).

Two tables of modelled data for the northern and southern segments include 2,626 observations for the southern segment obtained through 13 profiles, and 3,030 samples received from the 15 profiles for the northern segment. The dataset comprised the depths and coordinates for the measured profiles of the model data of each segment. The "psxy" module was used to plot graphs of the modelled profiles (Fig. 7) to feature geomorphology ranges. The resulting two graphs are shown in Figure 7. The 3D model (Fig. 5) was plotted using the "grdview" GMT model to visualise the trench in a three-dimensional cross-transect. The principle of the "grdview" was in reading a 2-D grid file (the ETOPO5 raster grid was taken) and plotting a 3D perspective coloured mesh plot by drawing a mesh topographic surface made up of rhomboid polygons over the geoid image.

Plotting statistical graphs is one of the methods used for better understanding the data distribution and variations within datasets. Data analysis in geospatial research can be performed using various tools and approaches, e.g. histograms, variation plots, ternary diagrams (Oshika et al. 2014; Saito and Tani 2017), spatial metrics (Klaučo et al. 2013b), 3D tomographic modelling of cross sections (Miller et al. 2005), geodynamic modelling of geological data (Faccenna et al. 2018), geostatistical assessment and analysis (Klaučo et al. 2013a), linear regressions and graphs of variables plotted against each other to visualise correlations in geological datasets (Lindh 2000, 2004; Lindh et al. 2000; Lemenkova 2019d, e), geospatial analysis (Suetova et al. 2005b), ecological assessment (Klaučo et al. 2014), and clustering (Lemenkova 2019h), to mention a few. A combination of various approaches for data analysis may result in comprehensive data interpre-

tation by means of statistical libraries and programming tools (Lemenkova 2019g).

From the variety of all existing methods of data analysis and statistical interpretation, it is necessary to select the most appropriate in the particular case study that would highlight the trends in data distribution given the limited size and scope of the research. Therefore, plotting of histograms (Fig. 8) was selected as the optimal tool to demonstrate depth distribution along the two segments of the hadal trench using the "ps histogram" GMT module. The methodology explained in GMT manuals (Wessel et al. 2019) was selected and followed stepwise. The core approach of the histogram plotting by GMT consists in the following. The "pshistogram" examines the selected data column from the file generated in the previous step (a table that contains depths and lat/lon coordinates of the cross-section profiles).

The statistical analysis of the trends of slope gradients for segments was done by the module "trend1d". The primary concept of these investigations is to visualise the plotted median bathymetric curve in two segments (Fig. 9) along the cross-section of 400 km and the curvature of the profile shape approximated by three mathematical functions (Huber 1964; Menke 1989; Smith and Wessel 1990). Cross-sections through the surfaces are pro-

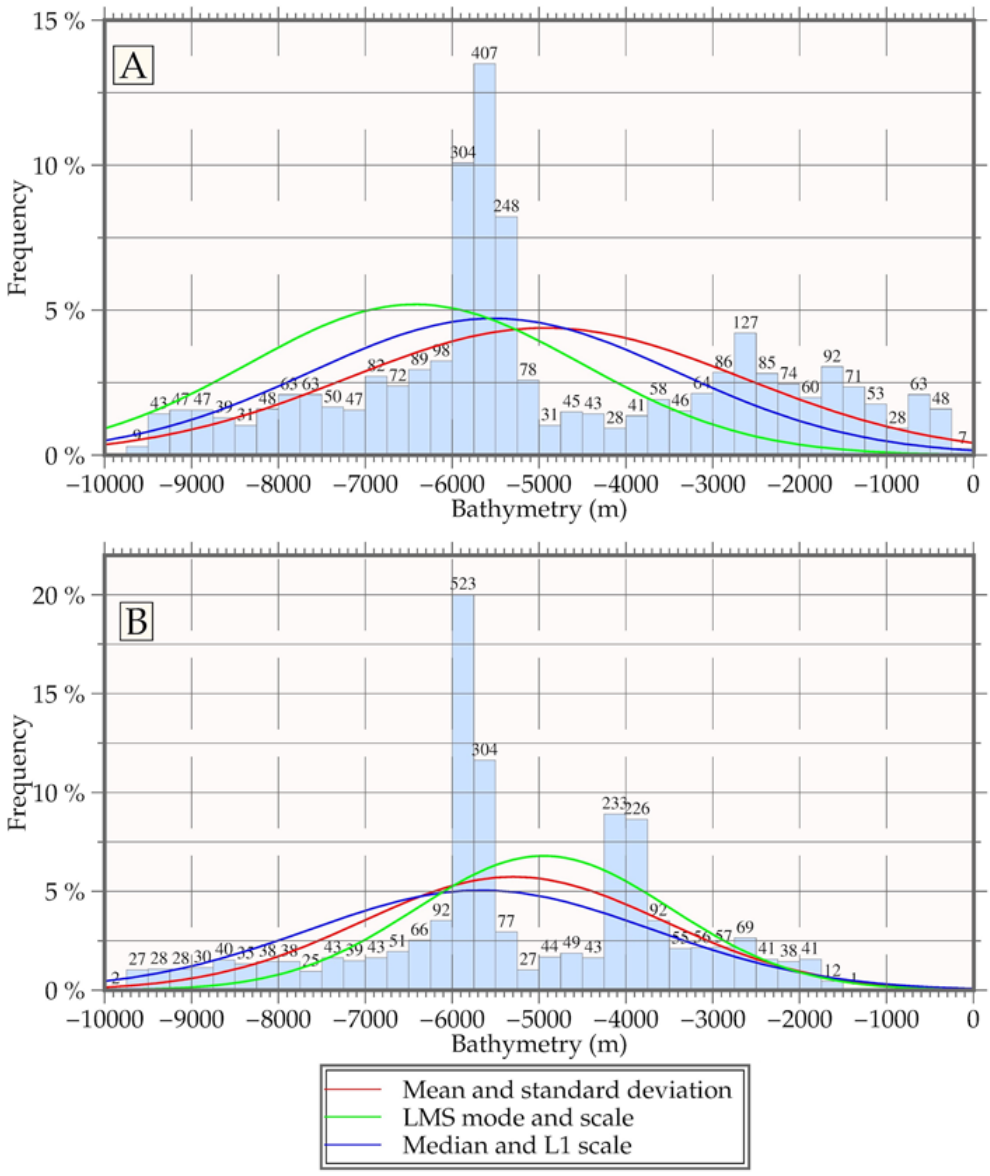

Fig. 8. Histograms showing depth distribution in two segments of the Izu-Bonin Trench

 Citation: Bulletin of Geography. Physical Geography Series 2020, 18, http://dx.doi.org/10.2478/bgeo-2020-0004

duced with splines in tension, which fits a regression model [y = f(x) + e] by weighted least squares (Wessel et al. 2019). The functional form of f(x) was chosen as polynomial (Ahlberg et al. 1967; de Boor 1978) and Fourier (Bracewell 1978), using the following formulae:

1. variant, Figure 9E: Basic LS line y = a + bx: gmt trend1d -Fxm stackIBTn.txt -Np1 > model.txt (the '-F' flag shows a single Fourier component);
2. variant, Figure 9D: Basic LS line y = a + bx + cx^2: gmt trend1d -Fxm stackIBTn.txt -Np2 > model.txt (an intermediate case using some tension. Here the "-Np2" flag shows polynomial with intercept and powers of 2. In the 2D case, the minimum-curvature method is the natural bicubic spline (Smith and Wessel 1990);
3. variant, Figure 9C: Basic LS line y = a + bx + cx^2 + spatial change gmt trend1d -Fxmr stackIBTn.txt -Np2,f1+l1 > model.txt (here "f1"is a Fourier series; "l" flag signifies length of modifiers; "xmr" signify x = x axis, m = model f(x), r = residual, used by GMT);
4. residuals, Figure 9B, the difference between the observed and predicted values of the bathymetric depth variable (z);
5. the original plot showing median stacked profile with error bars, Figure 9A.

The output file was saved in an ASCII format (model.txt) of numerical data and visualised in Figure 9.

Visual variations in approximated curvature of the seabed bottom cross-section profile correlate with the total stored elastic strain energy in the flexed plate, which is proportional to the curvature (Smith and Wessel 1990). As demonstrated, curvature of the topographic cross-sectioned seabed can be modelled conveniently by the functionality of the GMT using the "trend1d" module with embedded mathematical approximations of the data. In general cases, topographic surface roughness can be associated with local geological settings, and especially with tectonic plates' movements. Nevertheless, re-

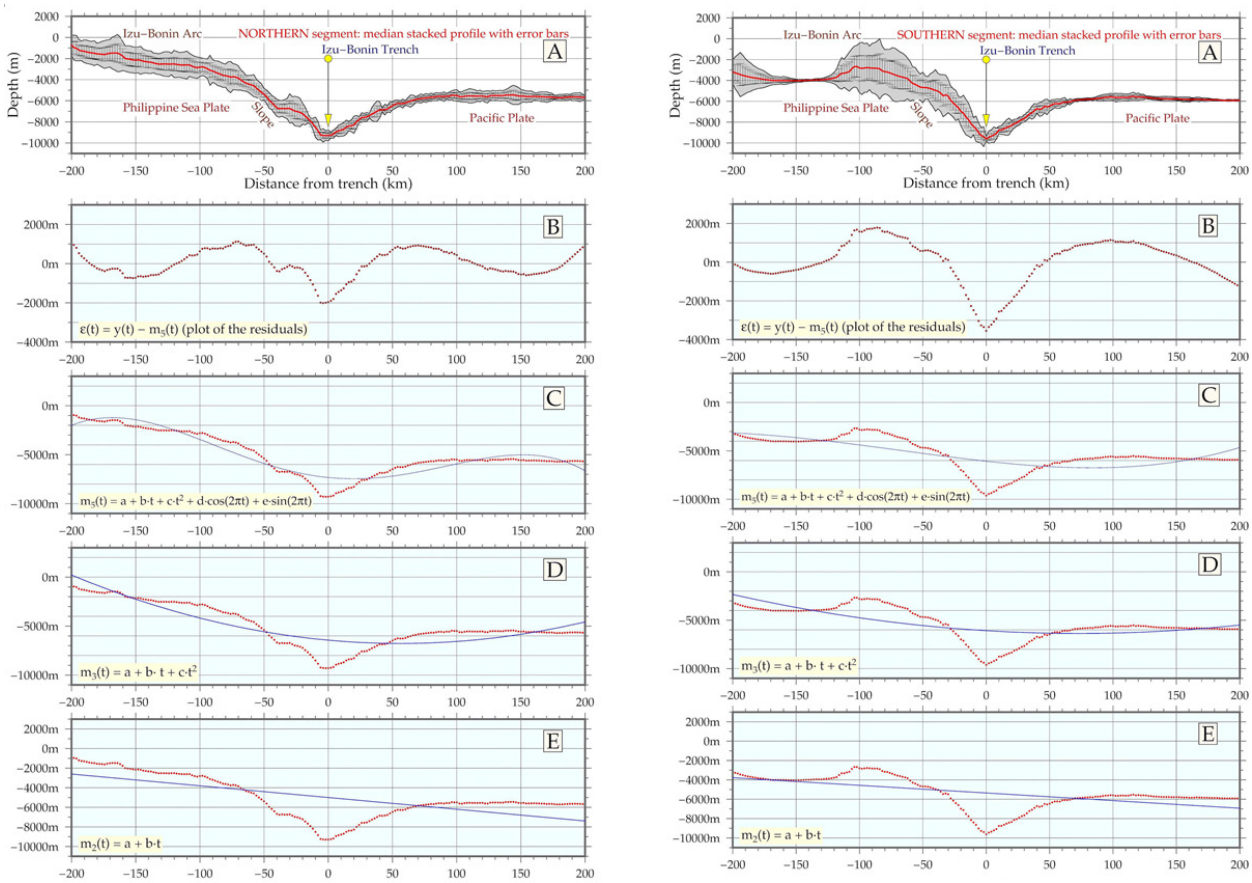

Fig. 9. Modelled trend curves of the gradient slopes in two segments, Izu-Bonin Trench

lationships between submarine topography, geomorphology and geologic conditions have a more complex nature and are still a topic for future research.

Results

The cross-sections are visualised as two segments of the Izu-Bonin Trench (Fig. 6). The results of the modelling demonstrated that the southern segment of the trench is deeper and is more precisely V-shaped with a steeper gradient slope on both slopes (Fig. 7B). The northern part of the trench (Fig. 7A) has asymmetric slopes with a notable submarine terrace on the western part and a more straight shape on the oceanward side (Fig. 7A). Furthermore, the southern segment of the trench has the Bonin Ridge distinguishable on the graph. The comparison of the oceanward flank of both segments of the Izu-Bonin Trench shows similar geomorphic shapes, but with seamounts on the northern part (Fig. 7). The 3D model of the Izu-Bonin shows (Fig. 5) seamounts (exaggerated for better visual effects) on the eastern part of the model. The trench is coloured deep purple with a general profile view on the grey draping border.

Most of the seafloor in the northern segment course is characterised by a flat-shaped bottom (Fig. 7A). This is most evident between -10 and 5 m in a horizontal cross-section, where the left-flank slope has a gradient of 61° while the right-flank slope gradient does not exceed 33°. A submarine terrace in the western wall can be identified at -6,800 m (Fig. 7A). The eastern flank of the Izu-Bonin Trench has a more homogeneous slope with occasional seamounts where it is slightly incised in contrast with the western segment. In the first 100 km of the horizontal cross-section, the profile of the northern segment of the trench (Fig. 7A) varies by no more than 3 km in depth (from -6,000 to -9,000 m) and shows slightly more complex geomorphology (compare Fig. 7A and 7B).

By contrast, the southern segment of the trench (Fig. 7B) presents a clear V-shaped axis, as can be seen in a segment of the cross-section at -6,000 to -9,500 m depth with the western flank clearly sharper (57.5°) than the eastern flank (39°). Its western wall (corresponding to the northern wall in the rest of the canyon) climbs almost 4 km (from -9,500 to -5,500 m) in barely 30 horizontal kilometres (Fig. 7B, western flank). At the distance of -120 km in a horizontal plan (Fig. 7B) at -4,100 m depth following the Bonin Ridge, the trench abruptly widens and opens onto the plain part until a gradual increase at -180 km in a horizontal transect (Fig. 7B, western flank). This, the Bonin Ridge, dissects the western wall of the southern segment of the trench into two distinct topographic parts. The southern segment (Fig. 7B), including all these topographic fluctuations, is up to 80 km wide in its deepest part, with a clearly asymmetric shape (50 km for the eastern flank and 30 km for the western flank), and has a V-shaped morphology.

The statistical analysis of the two segments shows the following results (Fig. 8). For the northern segment (Fig. 8A) for the most illustrative range of depths (that is from -5,000 to -6,000m), the northern segments shows a total of 1,037 recorded samples (304, 407, 248 and 78). The southern segment shows (Fig. 8B) a total of 931 samples (523, 304, 77 and 27). Furthermore, the histogram for the southern segment has a clear bimodal distribution with two peaks: 523 samples taking 20% show the most frequent depth values for the southern segment that lie in the range of -5,800 to -6,000m. The 2nd peak takes almost 10% of the data pool correlating with the Bonin Ridge location. These are the data in the range from -4,200 to -3,800 m. For the northern segment, the most repetitive samples (407 values, 13.5%) are taken by the depths from -5,600 to -5,800 m, followed by depths in the range -5,800 to -6,000 m (304 samples with 10%). In the northern segment, the data distribution has more samples located on shallow areas (146 recorded observations) pointing at the Izu-Bonin Arc, while for the southern segment there are no data recorded in this bathymetric range. That means that the southern segment has a more V-shaped trench profile, as is visible in Figure 7.

The presented topographic mapping of the Izu-Bonin Trench reveals differences in the bottom morphology of its two distinct segments, and reveals variations in submarine landforms that can be attributed to geological settings, rock composition, erosional processes, and transport and deposition of marine sediments. Interaction between geolog-

 Citation: Bulletin of Geography. Physical Geography Series 2020, 18, http://dx.doi.org/10.2478/bgeo-2020-0004

ic, tectonic and sedimentary processes, geochemical rock properties with trench formation and its topographic evolution are the main factors affecting its topography, which is presented as the models of subsequent cross-section profiles (Fig. 7). Other mechanisms driving the morphological differences between the two segments may include the following: (1) transported marine sediments; (2) more or less frequent sediment failure from the trench's slopes; (3) closer location to the island arc (western flank) and (4) submarine erosion.

Discussion

Submarine geomorphological and bathymetric mapping plays a critical role in analysis of marine benthic habitats, navigation, modelling marine environments, and other aspects. Therefore, testing new cartographic methods is important for further development of geospatial ocean modelling. This study has shown that the combination of GEBCO and the Earth Gravitational Models (EGM96) geoid data can support GMT-based thematic (topographic, geological and geophysical) mapping, 2D and 3D modelling of the submarine geomorphology of oceanic trenches to complement geospatial methods, and the use of statistical analysis for interpreting the results of bathymetric data processing. The presented study contributes to the methodological testing and application of the GMT scripting toolset algorithms for seafloor modelling and mapping.

As a recommendation for future studies, similar research can be upscaled or tested in other segments of oceanic trenches using other available geographic datasets. For instance, extraction of the specific submarine landform elements from a GEBCO or SRTM DEM can be detailed for the next level of abstraction and at a larger scale using information on landform types. Recognising submarine landform elements involves more detailed analysis of the selected slopes of the trench into facets along a bathymetric sequence from the submarine terraces to the trench bottom. Further modelling methods could test topographic variations along other segments of the trench.

Frequently, topographic variations lead to the formation of geomorphic forms that can be visualised in both the thematic map and as a 3D overlay with a topographic map. Some issues require further investigation – specifically for cartographic modelling of the trench. For example, a technical GMT issue of the cross-section technique for visualising a segment of a trench currently requires a straight line between the start and the end points of the segment. Therefore, the technique needs to be applicable to curved lines of a trench in order to provide a complete approach. The relationships between the submarine topography, geomorphology and geological and tectonic variations are not fully clarified as a model that could also be mathematically developed.

Based on the availability of data, additional geomorphometric elements can be studied: aspect, profile curvature, mean curvature of the cross-section profiles of the oceanic trenches. Variation in topographic forms also includes differences in seafloor morphology, which includes the system of canyons and depression connected to a trench and contributing to sediment upbringing. These geomorphic elements can be included in spatial analysis related to the bathymetric mapping. Furthermore, besides cartographic approaches to GMT, other machine learning techniques can be tested for advanced data analysis in geographic and geological modelling. Thus, it is recommended to apply scripting programming languages for geospatial data analysis that include: S (Pebesma 2004), C++ (Barillec et al. 2011), Python (Lemenkova 2019c), R (Lewin-Koh et al. 2002; Pebesma and Bivand 2005; Bivand et al. 2008; Lemenkova 2018b, c), or SPSS IBM Statistics for data analysis (Lemenkova 2019f).

The long-term aim for machine-learning programming applications in seafloor modelling is to develop a computational model of the geomorphic similarity of the trench shape based on a spatial analysis of the topographic cross-sectional profiles in its different segments. Currently, despite how important analysing topographic variation is for assessing geomorphological patterns, there exists no comprehensive automated method for modelling 3D curved profiles based on freeform surfacing using tangential continuity. Hence, mathematical approaches (Bézier, splines) can facilitate models of topographic variations. Besides this, geomorphic similarity between the patches of seafloor could be assessed using fractal-based geomorphometric the-

ory in a machine-learning approach (e.g. embedded in a GRASS GIS). The resulting model would account for those aspects of geologic and geochemical similarity that are based on the distribution of various rock types and sediments within the study area.

Conclusion

Bathymetric data, cross-section profiles, and thematic mapping (geological and geophysical data) were used to identify two coexisting topographic patterns in the southern and northern segments of the Izu-Bonin arc–trench system. The V-shaped deep southern part of the trench is the end result of the geochemical diversity caused by complex geological and tectonic processes exposed in the Izu Collision Zone (ICZ) that in the end affects topographic shape through collision-induced transformation from juvenile oceanic arc to mature continental crust in an ongoing arc–arc collision zone. As a result, the ICZ granitoid plutons are characterised by a wide range of geochemical diversity in spite of their geographical closeness (Tani 2011).

Differences in local geodynamic settings that caused the formation of various types of granitoid magmas in the ICZ led to the formation of various types of granitoid plutons ranging from tonalites and trondhjemites to granodiorites, monzogranites and granites (Saito and Tani 2017). Thus, according to the hybrid crust model (Saito et al. 2007), the detected elements include magmas of individual plutons within the granitic complex, the Honshu arc crustal metamorphosed terrigenous clastic sedimentary rocks and the subducted Izu-Bonin arc basaltic rocks under the ICZ. Since hydrothermal mineral alteration with relation to temperatures and geochemical content are the dominant factors in resistivity of rocks, the geological settings necessarily play an important role in geomorphic submarine landforms.

As a consequence, the geochemical diversity and such complex geological settings of the seafloor result in topographic variations of the Izu-Bonin Trench, which is reflected in the bottom morphological system. In addition, bathymetric variations affect the distribution of sediments eroded from the island arcs eastwards and directed towards the trench, with additional lateral supply of sediment inflow from minor submarine canyons. Such a complex network pattern of sediment distribution illustrates the contribution of canyons in transporting terrestrial sediments from the island arc, coastal and shelf areas via oceanic currents and the system of submarine landforms to the bottom of the trench, where they contribute to forming new landforms and gradually changing the submarine topography.

The set of cross-sectional topographic profiles obtained from the two segments along the Izu-Bonin Trench, together with geological analysis of the local and regional settings in the study area based on published data on geochemical and tectonic processes in the Izu-Bonin arc–trench subduction system, allows the following conclusions to be drawn regarding the differences in topography and bottom morphology of the trench in its northern and southern segments:

1. The different geochemical compositions of the underlying rocks, geology, volcanic activities and tectonic settings near Sagami Trough (northern segment) and Bonin Ridge (southern segment) and the earthquake activities near the Boso Triple Junction (northern segment) have an important impact on the topographic shape of the submarine landforms;
2. Tectonic processes involving subduction of plates have different rates in its northern (9 cm/yr) and central segment (6 cm/yr), decreasing southwards. This is reflected in the strong, destructive earthquakes common in central Japan (the northern part of the study area). Since the process of the trench's formation is induced by the convergence of two oceanic plates (the Pacific Plate is subducted under the Philippine Sea Plate at the Izu-Bonin Trench) variations in the tectonic plate movements necessarily affect the submarine topography of the trench.
3. The heterogeneity of physical properties in the subducted slabs have previously been discussed (Kennett and Gorbatov 2004). The tectonic history causes differences in the physical properties of the seafloor, which is explained by a combination of factors: variations in the age, rigidity and strength of

 Citation: Bulletin of Geography. Physical Geography Series 2020, 18, http://dx.doi.org/10.2478/bgeo-2020-0004

the subducting Pacific Plate in the mantle. Thus, Conrad and Hager (1999) noted that as the fault zone strength increases, the plate velocity decreases, since increased resistance in the fault zone slows the plate.

4. The geology of the Ogasawara Plateau causes heterogeneity in the regional bottom morphology. A seismic survey detected a topographic high (2,000–3,000 m) above the Izu-Bonin seafloor consisting of a series of seamounts (guyots) of Cretaceous age (Okamura et al. 1992). The flat summits of the guyots are filled with carbonate-rich lagoon sediments that are released into the mantle from the seamounts extending down into the subduction zone (Kerrick and Connolly 2001) which explains the low seismic velocity zone beneath the southern Izu-Bonin arc (Miller et al. 2004).

As briefly summarised above, the topographic shape of the trench is deeply connected with the physical rock properties and geochemistry, which in turn resulted from the tectonic plate movements. Therefore, modelling topographic variation of deep-sea trenches needs to include analysis and mapping of its geophysical and geological properties and tectonic regional settings, since these have a crucial role in indirectly affecting various factors (petrophysics, geology). As demonstrated above, the topography of the Izu-Bonin Trench varies in its different segments experiencing the effects of the set of geological factors and complex processes within the oceanic system.

Disclosure statement

No potential conflict of interest was reported by the author.

Acknowledgement

The research was funded by China Scholarship Council (CSC), State Oceanic Administration (SOA), Marine Scholarship of China, Grant Nr. 2016SOA002, People's Republic of China.

The author used the GMT software. The Generic Mapping Tools, GMT, are an open source collection of tools for manipulating geographic and Cartesian data sets (including filtering, trend fitting, gridding, projecting, etc.) and producing PostScript illustrations ranging from simple x–y plots via contour maps to artificially illuminated surfaces and 3D perspective views. It is released under the GNU Lesser General Public License (Wessel et al. 2019).

References

AHLBERG JH, NILSON EN and WALSH JL, 1967, The theory of splines and their applications. *Mathematics in Science and Engineering* 38, New York and London.

ARAI R and IWASAKI T, 2014, Crustal structure in the north-western part of the Izu collision zone in central Japan. *Earth Planet Space* 66: 1-12.

ARCULUS RJ, ISHIZUKA O, BOGUS KA, GURNIS M, HICKEY-VARGAS R, ALJAHDALI MH, BANDINI-MAEDER AN, BARTH AP, BRANDL PA and DRAB L, 2015, A record of spontaneous subduction initiation in the Izu–Bonin–Mariana arc. *Nature Geoscience* 8(9): 728–733.

ARISA D and HEKI K, 2016, Transient crustal movement in the northern Izu-Bonin arc starting in 2004: A large slow slip event or a slow back-arc rifting event? *Tectonophysics* 68: 206–213.

BARILLEC R, INGRAM B, CORNFORD D and CSATÓ L, 2011, Projected sequential Gaussian processes: a C++ tool for interpolation of large datasets with heterogeneous noise. *Computers and Geosciences* 37(3): 295–309.

BARNES JD and STRAUB SM, 2010, Chorine stable isotope variations in Izu Bonin tephra: Implications for serpentinite subduction. *Chemical Geology* 272: 62–74.

BIVAND RS, PEBESMA EJ and GOMEZ-RUBIO V, 2008, *Applied Spatial Data Analysis with R*. Spring-

er-Verlag, New York. URL http://www.asdar-book.org/ (accessed: 15 *October* 2019).

BRACEWELL RN, 1978, *The Fourier transform and its applications*. McGraw-Hill International.

ČÍŽKOVÁ H and BINA CR, 2015, Geodynamics of trench advance: Insights from a Philippine-Sea-style geometry. *Earth and Planetary Science Letters* 430: 408–415.

CONRAD, CP and HAGER BH, 1999, Effects of plate bending and fault strength at subduction zones on plate dynamics. *Journal of Geophysical Research* 104, 17,551–17,571.

COX A, 1973, *Plate tectonics and geomagnetic reversal*. San Francisco, Freeman.

DE BOOR, C, 1978, *A practical guide to splines*. Springer-Verlag New York, Inc.

DEBARI SM, TAYLOR B, SPENCER K and FUJIOKA K, 1999, A trapped Philippine Sea plate origin for MORB from the inner slope of the Izu-Bonin trench. *Earth and Planetary Science Letters* 174: 183–197.

DOBSON PF, BLANK JG, MARUYAMA S and LIOU J, 2006, Petrology and geochemistry of boninite-series volcanic rocks, Chichi-Jima, Bonin Islands, Japan. *International Geology Review* 48(8), 669–701.

FACCENNA C, DI GIUSEPPE E, FUNICIELLO F, LALLEMAND S and VAN HUNEN J, 2009, Control of seafloor aging on the migration of the Izu-Bonin-Mariana trench. *Earth and Planetary Science Letters* 288: 386–398.

FACCENNA C, HOLT AF, BECKER TW, LALLEMAND S and ROYDEN LH, 2018, Dynamics of the Ryukyu/Izu-Bonin-Marianas double subduction system. *Tectonophysics* 746: 229–238.

GAUGER S, KUHN G, GOHL K, FEIGL T, LEMENKOVA P and HILLENBRAND C, 2007, Swath- bathymetric mapping. In: Gohl, K. The expedition Antarktis-XXIII/4 of the Research Vessel 'Polarstern' in 2006. *Berichte zur Polar- und Meeresforschung // Reports on Polar and Marine Research* 557: 38–45.

GEBCO Committee, 2016, General Bathymetric Chart of the Oceans (GEBCO) – from the coast to the deepest trench. *Hydro International. [Online magazine]* Available from: https://www.hydro-international.com/content/article/from-the-coast-to-the-deepest-trench 19/05/2016

GONG W, XING J and JIANG X, 2018, Heterogeneous subduction structure within the Pacific plate beneath the Izu-Bonin arc. *Journal of Geodynamics* 116: 1–12.

GORBATOV, A and KENNETT, BLN, 2003, Joint bulk-sound and shear tomography for Western Pacific subduction zones. *Earth and Planetary Science Letters*, 210: 527–543.

HASHIMA A, SATO T, SATO H, ASAO K, FURUYA H, YAMAMOTO S, KAMEO K, MIYAUCHI T, ITO T, TSUMURA N and KANEDA H, 2016, Simulation of tectonic evolution of the Kanto Basin of Japan since 1 Ma due to subduction of the Pacific and Philippine Sea plates and the collision of the Izu-Bonin arc. *Tectonophysics* 679: 1–14.

HELL B and JAKOBSSON M, 2011, Gridding heterogeneous bathymetric data sets with stacked continuous curvature splines in tension. *Marine Geophysical Research* 32: 493–501.

HUBER PJ, 1964, Robust estimation of a location parameter. *Annals of Mathematical Statistics* 35: 73–101.

ICHIYAMA Y, ITO H, HOKANISHI N, TAMURA A and ARAI S, 2017, Plutonic rocks in the Mineoka–Setogawa ophiolitic mélange, central Japan: Fragments of middle to lower crust of the Izu–Bonin–Mariana Arc? *Lithos* 282–283: 420–430.

ISHIZUKA O, UTO K and YUASA M, 2003, Volcanic history of the back-arc of the Izu–Bonin (Ogasawara) arc. In: Larter RD, Leat PT (eds), Intra-Oceanic Subduction Systems: Tectonic and Magmatic Processes. *Geological Society London Special Publications,* 187–205.

ISHIZUKA O, HICKEY-VARGAS R, ARCULUS RJ, YOGODZINSKI GM, SAVOV IP, KUSANO Y, MCCARTHY A, BRANDL PA and SUDO M, 2018, Age of Izu–Bonin–Mariana arc basement. *Earth and Planetary Science Letters* 481: 80–90.

KAMIMURA A, KASAHARA J, SHINOHARA M, HINO R, SHIOBARA H, FUJIE G and KANAZAWA T, 2002, Crustal structure study at the Izu-Bonin subduction zone around 31°N: implications of serpentinized materials along the subduction plate boundary. *Physics of the Earth and Planetary Interiors* 132: 105–129.

KAWATE S and ARIMA M, 1998, Petrogenesis of the Tanzawa plutonic complex, central Japan: exposed felsic middle crust of the Izu-Bonin-Mariana arc. *Island Arc* 7: 342–358.

KENNETT BLN and GORBATOV A, 2004, Seismic heterogeneity in the mantle-strong shear wave signature of slabs from joint tomography. *Physics of the Earth and Planetary Interiors* 146: 88–100.

KERRICK DM and CONNOLLY JAD, 2001, Metamorphic devolatilization of subducted marine sediments

and the transport of volatiles into the earth's mantle *Nature* 411: 293–296.

KLAUČO M, GREGOROVÁ B, STANKOV U, MARKOVIĆ V and LEMENKOVA P, 2017, Land planning as a support for sustainable development based on tourism: A case study of Slovak Rural Region. *Environmental Engineering and Management Journal* 2(16): 449–458.

KLAUČO M, GREGOROVÁ B, STANKOV U, MARKOVIĆ V and LEMENKOVA P, 2014, Landscape metrics as indicator for ecological significance: assessment of Sitno Natura 2000 sites, Slovakia. *In: Ecology and Environmental Protection. Proceedings of the Int'l Conference* (Belarusian State University, March 19–20, 2014). Minsk, Belarus: BSU Press, 85–90.

KLAUČO M, GREGOROVÁ B, STANKOV U, MARKOVIĆ V and LEMENKOVA P, 2013a, Determination of ecological significance based on geostatistical assessment: a case study from the Slovak Natura 2000 protected area. *Central European Journal of Geosciences* 5(1): 28–42.

KLAUČO M, GREGOROVÁ B, STANKOV U, MARKOVIĆ V and LEMENKOVA P, 2013b, Interpretation of Landscape Values, Typology and Quality Using Methods of Spatial Metrics for Ecological Planning. Poster at: *54th International Conference Environmental and Climate Technologies* (Riga Technical University, Oct. 14, 2013). Riga, Latvia.

KUHN G, HASS C, KOBER M, PETITAT M, FEIGL T, HILLENBRAND CD, KRUGER S, FORWICK M, GAUGER S and LEMENKOVA P, 2006, The response of quaternary climatic cycles in the South-East Pacific: development of the opal belt and dynamics behavior of the West Antarctic ice sheet. In: Gohl K. (ed.) *Expeditionsprogramm Nr. 75 ANT XXIII/4, AWI Helmholtz Centre for Polar and Marine Research*, Bremerhaven, Germany.

LEMENKOVA P, 2011, *Seagrass Mapping and Monitoring Along the Coasts of Crete, Greece*. M.Sc. Thesis. University of Twente, Netherlands.

LEMENKOVA P, 2018a, R scripting libraries for comparative analysis of the correlation methods to identify factors affecting Mariana Trench formation. *Journal of Marine Technology and Environment* 2: 35–42.

LEMENKOVA P, 2018b, Hierarchical Cluster Analysis by R language for Pattern Recognition in the Bathymetric Data Frame: a Case Study of the Mariana Trench, Pacific Ocean. In: *Virtual Simulation, Prototyping and Industrial Design* 2(5): 147–152.

LEMENKOVA P, 2018c, Factor Analysis by R Programming to Assess Variability Among Environmental Determinants of the Mariana Trench. *Turkish Journal of Maritime and Marine Sciences* 4: 146–155.

LEMENKOVA P, 2019a, Scatterplot Matrices of the Geomorphic Structure of the Mariana Trench at Four Tectonic Plates (Pacific, Philippine, Mariana and Caroline): a Geostatistical Analysis by R. In: Degtyarev KE (ed.) Problems of Tectonics of Continents and Oceans. *Proceedings of the 51st Tectonics Meeting* 1: 347–352. RAS Institute of Geology. Moscow: GEOS.

LEMENKOVA P, 2019b, An Empirical Study of R Applications for Data Analysis in Marine Geology. *Marine Science and Technology Bulletin* 8(1): 1–9.

LEMENKOVA P, 2019c, Processing oceanographic data by Python libraries NumPy, SciPy and Pandas, *Aquatic Research* 2: 73–91.

LEMENKOVA P, 2019d, Testing Linear Regressions by StatsModel Library of Python for Oceanological Data Interpretation. *Aquatic Sciences and Engineerin*g 34: 51–60.

LEMENKOVA P, 2019e, Regression Models by Gretl and R Statistical Packages for Data Analysis in Marine Geology. *International Journal of Environmental Trends* 3(1): 39–59.

LEMENKOVA P, 2019f, Numerical Data Modelling and Classification in Marine Geology by the SPSS Statistics. *International Journal of Engineering Technologies* 5(2): 90–99.

LEMENKOVA P, 2019g, Statistical Analysis of the Mariana Trench Geomorphology Using R Programming Language. *Geodesy and Cartography* 45(2): 57–84.

LEMENKOVA P, 2019h, K-means Clustering in R Libraries {cluster} and {factoextra} for Grouping Oceanographic Data. *International Journal of Informatics and Applied Mathematics* 2(1): 1–26.

LEMENKOVA P, PROMPER C and GLADE T, 2012, Economic Assessment of Landslide Risk for the Waidhofen a.d. Ybbs Region, Alpine Foreland, Lower Austria. In: *Protecting Society through Improved Understanding. 11th International Symposium on Landslides and the 2nd North American Symposium on Landslides and Engineered Slopes NASL, June 2–8,* Banff, Canada, 279–285.

LEONT'EV OK, 1968, *The bottom of the ocean. Mys., Moscow.*

LEWIN-KOH NJ, BIVAND R, PEBESMA EJ, ARCHER E, BADDELEY A, BIBIKO HJ, DRAY S, FORREST D, FRIENDLY M, GIRAUDOUX P, GOLICHER D, RU-

BIO VG, HAUSMANN P, HUFTHAMMER KO, JAGGER T, LUQUE SP, MACQUEEN D, NICCOLAI A, SHORT T, STABLER B and TURNER R, 2012, *Maptools: Tools for Reading and Handling Spatial Objects. R package version 0.8-18,* URL http://CRAN.R-project.org/package=maptools (accessed: 15 October 2019).

LINDH P, 2000, Soil stabilisation offine-grained till soils – The effect of lime and hydraulic binders on strength and compaction properties. *Licentiate Thesis, Department of Geotechnology,* Lund University, Lund.

LINDH P, 2004, *Compaction- and strength properties of stabilised and unstabilised fine-grained tills.* PhD Thesis, Lund University, Lund.

LINDH P, DAHLIN T and SVENSSON M, 2000, Comparisons between different test methods for soil stabilisation. GeoEng 2000. *An international conference on geotechnical and geological engineering, Melbourne,* Nov. 19–24, 2000. 6.

LITVIN VM, 1987, *Morphostructure of the ocean seafloor.* Nedra, Leningrad.

MENKE W, 1989, *Geophysical Data Analysis: Discrete Inverse Theory,* Revised Edition, Academic Press, San Diego.

MILLER MS, GORBATOV A and KENNETT BLN, 2005, Heterogeneity within the subducting Pacific slab beneath the Izu-Bonin-Mariana arc: Evidence from tomography using 3D ray tracing inversion techniques. *Earth and Planetary Science Letters* 235: 331–342.

MILLER MS, KENNETT BLN and LISTER GS, 2004, Imaging changes in morphology, geometry, and physical properties of the subducting Pacific Plate along the Izu–Bonin–Mariana Arc. *Earth and Planetary Science Letters* 224: 363–370.

NAKAJIMA K and ARIMA M, 1998, Melting experiments on hydrous low-K tholeiite: implications for the genesis of tonalitic crust in the Izu–Bonin–Mariana arc. *The Island Arc* 7: 359–373.

NIITSUMA N, 1989, Collision tectonics in the south Fossa Magna, Central Japan. *Modern Geology* 14: 3–18.

NISHIZAWA A, KANEDA K, NAKANISHI A, TAKAHASHI N and KODAIRA S, 2006, Crustal structure of the ocean-island arc transition at the mid Izu-Ogasawara (Bonin) arc margin. *Earth Planets Space* 58: e33–e36.

OGAWA Y, SENO T, TOKUYAMA H, AKIYOSHI H, FUJIOKA K and TANIGUCHI H, 1989, Structure and development of the Sagami trough and the Boso triple junction. *Tectonophysics* 160: 135–150.

OKAMURA Y, MURAKAMI F, KISHIMOTO K and SAITO E, 1992, Seismic profiling survey of the Ogasawara Plateau and Michelson Ridge, Western Pacific: evolution of cretaceous guyots and deformation of a subducting oceanic plateau. *Bulletin of the Geological Survey of Japan* 43: 237–256.

OSHIKA J, ARAKAWA Y, ENDO D, SHINMURA T and MORI Y, 2014, A rare basanite distribution in the northern part of the Izu–Bonin volcanic arc, Japan: Petrological and geochemical constraints. *Journal of Volcanology and Geothermal Research* 270: 76–89.

OTOFUJI Y, KAMBARA A, MATSUDA T and NOHDA S, 1994, Counterclockwise rotation of Northeast Japan: Paleomagnetic evidence for regional extent and timing of rotation. *Earth and Planetary Science Letters* 121: 503–518.

PEBESMA EJ, 2004, Multivariable geostatistics in S: the gstat package. *Computers and Geoscience* 30: 683–691.

PEBESMA EJ and BIVAND RS, 2005, Classes and Methods for Spatial Data in R. R News, 5(2): 9–13. URL http://CRAN.R-project.org/doc/Rnews/ (accessed: 15 *October* 2019).

PEYVE AV, 1980, *Geology of the bottom of the Philippine Sea*. Science, Moscow.

REAGAN MK, ISHIZUKA O, STERN RJ, KELLEY KA, OHARA Y, BLICHERT-TOFT J, BLOOMER SH, CASH J, FRYER P and HANAN BB, 2010, Fore-arc basalts and subduction initiation in the Izu–Bonin–Mariana system. *Geochemistry, Geophysics, Geosystems* 11(3): 1-17

RODNIKOV AG, 1979, *Island arcs of the western part of the Pacific Ocean*. Nauka, Moscow.

SAITO S and TANI K, 2017, Transformation of juvenile Izu–Bonin–Mariana oceanic arc into mature continental crust: An example from the Neogene Izu collision zone granitoid plutons, Central Japan. *Lithos* 277: 228–240.

SAITO S, ARIMA M, NAKAJIMA T, MISAWA K, KIMURA JI, 2007, Formation of distinct granitic magma batches by partial melting of hybrid lower crust in the Izu arc collision zone, Central Japan. *Journal of Petrology* 48: 1761–1791.

SAITO S, ARIMA M, NAKAJIMA T, TANI K, MIYAZAKI T, SENDA R, CHANG Q, TAKAHASHI T, HIRAHARA Y and KIMURA JI, 2012, Petrogenesis of the Kaikomagatake granitoids pluton in the Izu collision zone, Central Japan: implications for transformation of juvenile oceanic arc into mature continental

crust. *Contributions to Mineralogy and Petrology* 163: 611–629.

SANDWELL DT, MÜLLER RD, SMITH WHF, GARCIA E and FRANCIS R, 2014, New global marine gravity model from CryoSat-2 and Jason-1 reveals buried tectonic structure. *Science* 346(6205): 65–67.

SANO T, SHIRAO M, TANI K, TSUTSUMI Y, KIYOKAWA S and FUJII T, 2016, Progressive enrichment of arc magmas caused by the subduction of seamounts under Nishinoshima volcano, Izu–Bonin Arc. *Japan Journal of Volcanology and Geothermal Research* 319: 52–65.

SCHENKE HW and LEMENKOVA P, 2008, Zur Frage der Meeresboden-Kartographie: Die Nutzung von AutoTrace Digitizer für die Vektorisierung der Bathymetrischen Daten in der Petschora-See. *Hydrographische Nachrichten* 25(81): 16–21.

SENDA R, SHIMIZU K and SUZUKI K, 2016, Ancient depleted mantle as a source of boninites in the Izu-Bonin-Mariana arc: Evidence from Os isotopes in Cr-spinel and magnetite. *Chemical Geology* 439: 110–119.

SMITH WHF, 1993, On the accuracy of digital bathymetric data. *Journal of Geophysical Research* 98(B6): 9591–9603.

SMITH WHF and SANDWELL DT, 1995, Marine gravity field from declassified Geosat and ERS-1 altimetry. *EOS Transactions American Geophysical Union* 76: Fall Mtng Suppl, F156.

SMITH WHF and WESSEL P, 1990, Gridding with continuous curvature splines in tension. *Geophysics* 55: 293–305.

SOH W, PICKERING KT, TAIRA A and TOKUYAMA H, 1991, Basin evolution in the arc–arc Izu collision zone, Mio-Pliocene Miura group, Central Japan. *Journal of Geological Society* 148: 317–330.

SOH W, NAKAYAMA K, and KIMURA T, 1998, Arc–arc collision in the Izu collision zone, Central Japan, deduced from the Ashigara Basin and adjacent Tanzawa Mountains. *The Island Arc* 7: 330–341.

STERN RJ, FOUCH MJ, KLEMPERER S, 2003, An Overview of the Izu-Bonin-Mariana Subduction Factory. In: Eiler J. (ed.), Inside the Subduction Factory. *American Geophysical Union Monograph* 138: 175–222.

SUETOVA IA, USHAKOVA LA and LEMENKOVA P, 2005a, Geoinformation mapping of the Barents and Pechora Seas. *Geography and Natural Resources* 4: 138–142.

SUETOVA I, USHAKOVA L and LEMENKOVA P, 2005b, Geoecological Mapping of the Barents Sea Using GIS. *Proceedings of the International Cartographic Conference ICC*. July 9–16, La Coruna, Spain.

TAKAHASHI M and SAITO K, 1997, Miocene intra-arc bending at an arc–arc collision zone, Central Japan. *The Island Arc* 6: 168–182.

TAMURA Y, ISHIZUKA O, AOIKE K, KAWATE S, KAWABATA H, CHANG Q, SAITO S, TATSUMI Y, ARIMA M, TAKAHASHI M, KANAMARU T, KODAIRA S, and FISKE RS, 2010, Missing Oligocene crust of the Izu-Bonin arc: consumed or rejuvenated during collision? *Journal of Petroleum Science and Engineering* 51: 823–846.

TANI K, 2011, Crustal Development of Intra-Oceanic Arc and Arc–Arc Collision Zone: Geochronological and Geochemical Study of Izu-Bonin Arc and Izu Collision Zone. *PhD Thesis*, Yokohama National University, Japan.

TAYLOR B, 1992, Rifting and the volcanic–tectonic evolution of the Izu–Bonin–Mariana arc. In: Taylor B, Fujioka K et al. (eds), *Proc. ODP, Sci. Results, 126. Ocean Drilling Program, College Station*, TX, 627–651.

TOLLSTRUP D, GILL J, KENT A, PRINKEY D, WILLIAMS R, TAMURA Y and ISHIZUKA O, 2010, Across-arc geochemical trends in the Izu-Bonin arc: contributions from the subducting slab, revisited. *Geochemistry, Geophysics, Geosystems* 11(1): 1-27.

TUEZOV IK, 1978, *The main features of the geological structure of the bottom of the Sea of Japan*. Nauka, Moscow.

UDINTSEV GB, 1972, *Geomorphology and tectonics of the bottom of the Pacific Ocean*. Nauka, Moscow.

WEATHERALL P and CRAMER R, 2004, The Bottom Line – Studying the contours of the ocean floor. *Planet Earth* (NERC publication).

WEATHERALL P, MARKS K and JAKOBSSON M, 2016, *Proc. International Conference on Marine Data and Information Systems (IMDIS)*, Gdansk, Poland. Global bathymetric data sets – (GEBCO) October 2016.

WESSEL, P, LUIS JF, UIEDA L, SCHARROO R, WOBBE F, SMITH, WHF AND TIAN D, 2019, The Generic Mapping Tools version 6. *Geochemistry, Geophysics, Geosystems*, 20: 5556–5564. DOI: https://doi.org/10.1029/2019GC008515

WESSEL P and SMITH WHF, 1998, New, improved version of the generic mapping tools released. *EOS Transactions American Geophysical Union* 79: 579.

WESSEL P and SMITH WHF, 2018, *The Generic Mapping Tools. Version 4.5.18 Technical Reference and Cookbook* (Computer software manual). U.S.A.

WESSEL P, SMITH WHF, SCHARROO R, LUIS JF and WOBBE F, 2013, Generic mapping tools: improved version released. *EOS Transactions American Geophysical Union* 94(45): 409–410.

WESSEL P, SMITH WHF, SCHARROO R, LUIS J and WOBBE F, 2019, *The Generic Mapping Tools. GMT Man Pages. Release 5.4.5* (Computer software manual). U.S.A. 504.

WHITMAN JM, HARRISON CGA and BRASS GW, 1983, Tectonic evolution of the Pacific Ocean since 74 Ma. *Tectonophysics* 99 (2–4): 241–249.

WOELKI D, REGELOUS M, HAASE KM, ROMER RHW and BEIER C, 2018, Petrogenesis of boninitic lavas from the Troodos Ophiolite, and comparison with Izu–Bonin–Mariana fore-arc crust. *Earth and Planetary Science Letters* 498: 203–214.

WYATT D, 2019, General Bathymetric Chart Of The Oceans (GEBCO) an IHO-IOC Joint Project. David. *Proc. 19th North Indian Ocean Hydrographic Commission (NIOHC) Meeting*, Muscat, Oman, 26–28 March 2019.

YAMAZAKI T, TAKAHASHI M, IRYU Y, SATO T, ODA M, TAKAYANAGI H, CHIYONOBU S, NISHIMURA A, NAKAZAWA T and OOKA T, 2010, Philippine Sea Plate motion since the Eocene estimated from paleomagnetism of seafloor drill cores and gravity cores. *Earth Planets Space* 62: 495–502.

ZHANG H, WANG F, MYHILL R and GUO H, 2019, Slab morphology and deformation beneath Izu-Bonin. *Nature Communications* 10(1310): 1–9. DOI: https://doi.org/10.1038/s41467-019-09279-7

Received 24 October 2019
Accepted 7 May 2020